Highlight Review

One-dimensional Halogen-bridged Ni^{III} Compounds: Chemistry and Physics in Strongly Correlated Electron Systems

Shinya Takaishi* and Masahiro Yamashita*

(Received December 25, 2007; CL-078013)

Abstract

In this review, we describe the structure, physical properties, and electronic structure of halogen-bridged one-dimensional (1D) Ni^{III} compound $[Ni(chxn)_2Br]Br_2$, which is one of the mostly studied 1D strongly correlated electron compounds. We also introduce recent progress of our study of Ni^{III} compounds.

♦ Introduction

One-dimensional (1D) halogen-bridged MX chains, in other words, Wolffram's red salt analogues have been extensively studied for more than 100 years as 1D mixed-valence systems, since Wolffram reported the first Cl-bridged platinum compound, $[Pt^{II}(NH_2C_2H_5)_4][Pt^{IV}(NH_2C_2H_5)_4Cl_2]Cl_4 \cdot 4H_2O$ in 1900.[1] These compounds form highly isolated 1D electron systems, such as –M–X–M–X– 1D linear chain structures, composed of the d_{z^2} orbitals of metal ions (M = Pd and Pt) and the p_z orbitals of bridging halide ions (X = Cl, Br, and I). Their mixed-valence structures $–X\cdots M^{II}\cdots X–M^{IV}–X\cdots$ (M = Pd and Pt; X = Cl, Br, and I) have been widely studied as 1D materials with strong electron–lattice-coupled systems. Since the 1970s, these compounds have been interested from the viewpoint of solid-state physics as 1D Peierls–Hubbard systems, where the electron–phonon interaction (S), the electron transfer (T), and the on-site and neighboring-site Coulomb repulsion energies (U and V, respectively) compete or cooperate with one another.[2] Their Peierls distorted 1D structure was noted as a charge-density-wave (CDW) state, and unique optical and dynamical properties such as intense and dichloic charge-transfer bands,[3] overtone progressions in resonant Raman spectra,[4] and luminescence with a large Stokes shift[5] as well as long-range migration of spin-solitons and polarons along 1-D chains[6] have been reported.

On the other hand, studies on the Ni compounds began in early 1980s.[7] In those days, there had been much controversy over their electronic structures.[7,8] Some groups insisted that these compounds are in a mixed-valence state ($–X\cdots Ni^{II}\cdots X–Ni^{IV}–X\cdots$), and other groups insisted that these compounds are in an averaged-valence state ($–X–Ni^{III}–X–Ni^{III}–X–$). The averaged-valence state of the compounds has been confirmed by crystal structure analysis,[9] X-ray photoelectron spectroscopy (XPS), and Auger electron spectroscopy (AES) of $[Ni(chxn)_2Br]Br_2$.[10] This is due to the larger U value ($\approx$5 eV) of the Ni compounds compared with those of Pd ($\approx$1.5 eV)[11] and Pt ($\approx$1.0 eV)[12] compounds. Therefore, the electronic state of these Ni^{III} compounds are noted as the Mott–Hubbard (MH) state, or Mott insulator. Physical properties of the Ni compounds have been extensively studied, and a lot of interesting properties, such as gigantic third-order nonlinear optical susceptibility ($\chi^{(3)}$),[13] quite strong antiferromagnetic interaction,[14] and spin-Peierls transition[15] have been reported. These compounds have been also interesting as a 1D model of high T_c copper oxide superconductors because the band structures of these compounds are quite analogous to La_2CuO_4, which is the mother compound of high T_c copper oxide superconductor $La_{2-x}Sr_xCuO_4$, except for their dimensionality.

In this review, we focus on the Ni^{III} system and introduce structure, physical properties, and recent progresses of the Ni^{III} compounds.

♦ Experimental

Halogen-bridged Ni^{III} compounds were synthesized by chemical (halogen vapor) or electrochemical oxidation of corresponding Ni^{II} species. Electrochemical oxidation usually affords better quality single crystals. A typical method is as follows: Nickel bromide anhydrate (2.2 mmol) is added to 4.0 mmol of $Ni(chxn)_3Br_2$ (chxn = 1*R*,2*R*-diaminocyclohexane) in 100 mL of anhydrous methanol. The mixture is refluxed for 6 h to obtain a blue-colored 60 mM methanol solution of $[Ni(chxn)_2]Br_2$. Tetra-*n*-butylammonium bromide (10 mmol) is added to the solution and the mixture was electrolyzed under constant current of 10 μA for two weeks. Black prismatic single crystals are obtained at the anode.

♦ Crystal Structure

Figure 1 shows crystal structures of the representative Ni^{III} compound $[Ni(chxn)_2Br]Br_2$.[9] $Ni(chxn)_2$ moieties are bridged by Br ions, forming a Ni–Br–Ni–Br linear chain along b axis. The crystal structure of this compound is isomorphous to the corresponding Pd and Pt compounds $[M(chxn)_2X]X_2$ (M = Pd and Pt; X = Cl, Br, and I). There is a marked difference between the Ni compound and the Pd or Pt compounds in the position of the bridging halide ions. In the present compound, bridging Br ions are located at the midpoint between neighboring Ni ions, whereas those are located at a displaced position from the midpoint in Pd or Pt compounds with disorder. This indicates that all Ni ions are crystallographically equivalent in the crystal, and the complex is in the Ni^{III} Mott–Hubbard state. Hydrogen

Shinya Takaishi[*1,2] *and Masahiro Yamashita*[*1,2]
[1]*Department of Chemistry, Graduate School of Science, Tohoku University, 6-3 Aza-Aoba, Aramaki Aoba-ku, Sendai 980-8578*
[2]*CREST, Japan Science and Technology Corporation, Kawaguchi 333-0012*
E-mail: yamasita@agnus.chem.tohoku.ac.jp

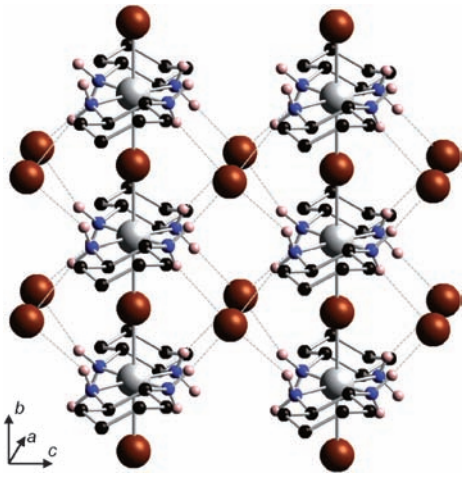

Figure 1. Crystal packing of $[Ni(chxn)_2Br]Br_2$. Dashed lines show hydrogen bonds. Hydrogen atoms bonding to carbon atoms are omitted for clarity. Gray: Ni, Brown: Br, Blue: N, Black: C, Pink: H.

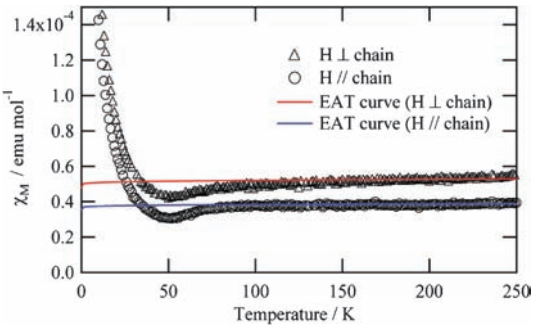

Figure 2. Magnetic susceptibilities observed in a single crystal of $[Ni(chxn)_2Br]Br_2$ with a magnetic field (1 T) parallel and perpendicular to the 1D chain. Red and blue lines show theoretical susceptibilities proposed by Eggert, Affleck, and Takahashi (EAT) with $J = 2000$ K.

bonds exist between amino protons and counter anions, forming a 2D network. Ni–Ni distances along the 1D chain are 5.161(2) and 5.157(1) Å at room temperature and $-152\,^{\circ}C$, respectively.

♦ Magnetic Properties

Figure 2 shows temperature dependence of magnetic susceptibility of $[Ni(chxn)_2Br]Br_2$ measured in a single crystal with a magnetic field of 1 T.[15] Temperature dependence of magnetic susceptibility showed Curie-like behavior at low temperature, and almost no temperature dependence at higher temperature. A small amount of spin concentration showing Curie-like behavior (≈0.4%) is attributed to some paramagnetic impurities or spins at the chain end. The weakly temperature-dependent susceptibility at high temperature is interpreted as that of an $S = 1/2$ Heisenberg chain with strong antiferromagnetic (AF) interaction. Such temperature dependence of susceptibilities can be understood by the Bonner–Fisher theory.[16] Recently, Eggert, Affleck, and Takahashi (EAT) have proposed theoretical susceptibility more accurately, which slightly differs from the Bonner–Fisher results in the behavior at low temperatures.[17] The result of EAT theory for $T < 0.2J/k_B$ is given by the following equation:

$$\chi(T) = \frac{Ng^2\mu_B{}^2}{2J\pi^2}\left\{1 + \frac{1}{2\ln(15.4\,J/k_BT)}\right\} \quad (1)$$

where the N is Abogadro's number, g is Lande's g factor, and k_B is the Boltzmann constant. In this equation, J is defined as $H = 2J\Sigma \boldsymbol{S}_i \cdot \boldsymbol{S}_{i+1}$. The exchange interaction was evaluated to be $J/k_B = 2000 \pm 500$ K by fitting the present data above 130 K to the EAT theoretical curve. The magnetic susceptibility slightly decreased below 100 K. This finding indicates some phase transition occurs to the nonmagnetic state, that is possibly CDW (–Br···Ni^{II}···Br–Ni^{IV}–Br···) or spin-Peierls states (···Br···Ni^{III}–Br–Ni^{III}···Br···).

To clarify possible transitions, we have measured the temperature dependence of the nuclear quadrupole resonance (NQR) signals of bridging Br ions because the NQR is a quite sensitive probe for detecting subtle changes in the electron distribution around NQR nuclei.

We observed a single resonance line for ^{81}Br at 300 K (137.079 ± 0.005 MHz) and a pair of lines $130.87_4 \pm 0.01$ and $147.78_6 \pm 0.01$ MHz at 3.8 K. We assigned these resonance signals to ^{81}Br nuclei by observing corresponding ^{79}Br lines at 164.091 ± 0.005 MHz (300 K), and $156.65_6 \pm 0.01$ and $176.90_4 \pm 0.01$ MHz (3.8 K) in good agreement with the reported isotope frequency ratio (^{79}Br/^{81}Br: 1.1969).[18] These resonance frequencies can be assigned to bridging Br atoms and not to counter Br ions, because ^{79}Br NQR frequencies in compounds with Ni–Br covalent bonds were observed in nearly the same frequency range, i.e., 126.26 MHz in $NiBr_2[P(C_3H_7)_3]_2$[19] and 126.53 MHz in $NiBr_2[P(C_4H_9)_3]_2$[19] at room temperature, whereas ionic Br ions mostly exhibit resonance lines[20] at frequencies of one order of magnitude lower than those in the present complex.

Figure 3 shows a temperature dependence of ^{81}Br NQR frequencies of the bridging Br in $[Ni(chxn)_2Br]Br_2$. A single ^{81}Br NQR line was observed at room temperature, being consistent with the X-ray diffraction work[9] that all bridging Br sites are equivalent at room temperature, i.e., $[Ni(chxn)_2Br]Br_2$ is in a Mott–Hubbard state. The fact that the resonance frequency gradually decreased with increasing temperature above 130 K is explained by the averaging of the electric field gradient (EFG) at Br nuclei by lattice vibrations. This temperature

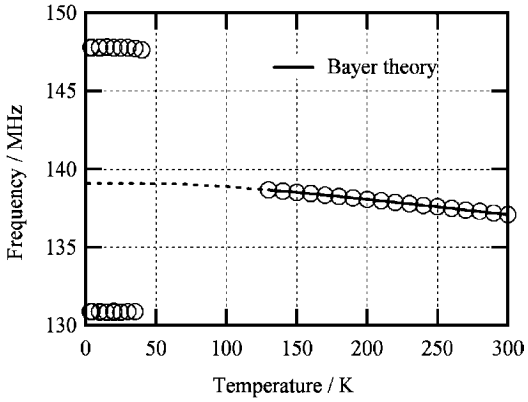

Figure 3. Temperature dependences of ^{81}Br NQR frequencies observed in $[Ni(chxn)_2Br]Br_2$. Dotted line is an extrapolation to 0 K according to the Bayer theory.

Published on the web (Advance View) March 15, 2008; doi:10.1246/cl.2008.382

dependence of the NQR frequency ($\nu(T)$) can be described by the harmonic oscillator model for lattice vibrations[21] and can be expressed as

$$\nu(T) = \nu_0\left[1 - A\coth\left(\frac{\hbar\omega}{2k_BT}\right)\right] \quad (2)$$

where ν_0, A, and ω are the resonance frequency for the static lattice, a coefficient depending on modes of lattice vibrations, and the averaged vibration frequency, respectively. The observed data were well fitted by eq 2, and the extrapolated frequency to 0 K was determined to be $\nu(0) = 139.1 \pm 0.2$ MHz.

Upon cooling, the NQR signal disappeared around 130 K, and two lines at 130.87 and 147.78 MHz appeared below ca. 40 K. The loss of resonance signals between 40 and 130 K is considered to be spectrum broadening attributable to the fluctuation of EFG by a phase transition. Since the averaged frequency of these two lines is almost the same as the frequency extrapolated from the high-temperature side, the NQR signals below 40 K are explained by the splitting of the high-temperature signal. Two resonance lines with a large frequency separation of 16.9 MHz at low temperatures indicate the presence of two nonequivalent Br sites, suggesting that some change of the electronic state in $[Ni(chxn)_2Br]Br_2$ takes place between 40 and 130 K.

Here, we discuss the possible electronic structures of the present compound. In the averaged valence (Mott–Hubbard) state, the environments of all Ni or bridging Br sites should be equivalent, resulting in a single Br NQR line. In the CDW state realized by displacement of bridging Br sites, environments of all Br sites are equivalent although two nonequivalent Ni sites exist, and, hence, this state affords a single Br NQR line. In the spin-Peierls state characterized by the displacement of Ni sites, however, two nonequivalent bridging Br sites are formed in good agreement with the two Br NQR lines. The splitting of NQR signals indicates that a spin-Peierls transition occurs in $[Ni(chxn)_2Br]Br_2$ in the range 40–130 K. This explanation is consistent with the decrease in the magnetic susceptibility observed below 100 K. As shown in Figure 2, χ observed in the low-temperature range below 100 K clearly deviated isotropically from the EAT curve. This decrease in χ is explainable by the spin cancellation caused by the transition into a spin-Peierls state.

The charge distribution in the Ni–Br bond can be evaluated by applying the Townes–Dailey approximation[22] given by

$$|e^2Qq| = (1 - i)(1 - s)|e^2Qq_{atom}| \quad (3)$$

where e^2Qq, e^2Qq_{atom}, i, and s denote the observed coupling constant given the twice the observed resonance frequency ($2h\nu$) by assuming axial symmetric EFG, the coupling constant in atomic ^{81}Br given by 643.032 MHz,[23] the extent of ionicity in the Ni–Br bond, and the s-character in the bonding orbital in Br, respectively. The s character, which is the contribution of the s orbital in the sp hybrid orbital in Br, was assumed to be 0.15 by Dailey and Townes[22] in cases when the halide ion is bonded to atoms more electropositive than the halide by as much as 0.25. Applying this approximation, partial electron-transfer values (i) from Ni to Br comparing with the value (0.0) in a neutral Br atom were evaluated to be 0.49_1 (high-temperature phase) and 0.52_1 and 0.45_9 (low-temperature phase). The extrapolated frequency of the high-temperature phase to 0 K ($\nu(0)$) was used to get the e^2Qq ($\approx 2\nu(0)$) in the high-temperature phase. The differences between i values in the high- and the low-temperature phases amounting to 0.03 are comparable to those among $i = 0.37$,[24] 0.38,[25] and 0.39[26] determined in octahedral complex ions $[MBr_6]^{2-}$ containing M–Br bonds where M = $Pd^{4+}(4d^6)$, $Pt^{4+}(5d^6)$, and $Re^{4+}(5d^3)$, respectively, suggesting that a marked change in the electronic population in Br atoms takes place through the spin-Peierls transition in the present complex.

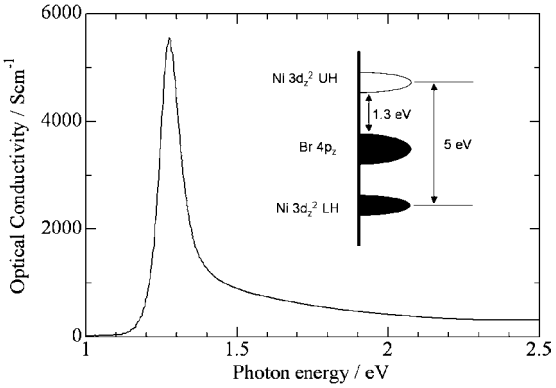

Figure 4. Optical conductivity spectrum of $[Ni(chxn)_2Br]Br_2$. Inset shows the band structure of $[Ni(chxn)_2Br]Br_2$.

♦ Optical Properties

Figure 4 shows the polarized optical conductivity spectrum ($E\|b$) of $[Ni(chxn)_2Br]Br_2$ obtained by the Kramers–Kronig transformation of the reflectivity spectrum, which corresponds to the absorption spectrum.[10] A sharp and intense absorption band was observed at 1.3 eV. The intense absorption spectra is also observed in Pd or Pt compounds, which are assignable to charge-transfer (CT) excitation from the fully occupied d_{z^2} orbital of the M^{II} site to the unoccupied d_{z^2} orbital of the nearest-neighbor M^{IV} site. In the present (Ni) case, on the other hand, the origin of the absorption band ought to be different from the Pd or Pt cases, because the ground state of Ni compounds are Ni^{III} Mott–Hubbard state.

Here, we consider the band structure of this compound. The half-filled d_{z^2} band of Ni splits because of the strong on-site Coulomb repulsion U ($\approx$5 eV), affording fully occupied lower-Hubbard (LH) band and unoccupied upper-Hubbard (UH) band. On the other hand, optical gap energy ($\approx$1.3 eV) is much smaller than U. Therefore, we can exclude the possibility that this intense band is attributed to the metal-to-metal charge-transfer (MMCT) band (Ni^{III},$Ni^{III} \rightarrow Ni^{II}$,$Ni^{IV}$). Although there had been controversy in attribution of the intense absorption band, it is now established that this band is attributed to bridging ligand (p_z band of Br^-) to metal (UH d_{z^2} band of Ni) charge-transfer (LMCT) band. Therefore, the band structure of this compound can be shown as inset of Figure 4.

The realization of all-optical switching, modulating, and computing devices is an important goal in modern optical technology. Nonlinear optical materials with large third-order nonlinear susceptibilities ($\chi^{(3)}$) are indispensable for such devices, because the magnitude of this quantity dominates device performance. A key strategy in the development of new materials with large nonlinear susceptibilities is the exploration of quasi-one-dimensional systems or quantum wires, because the quantum confinement of electron–hole motion in one-dimen-

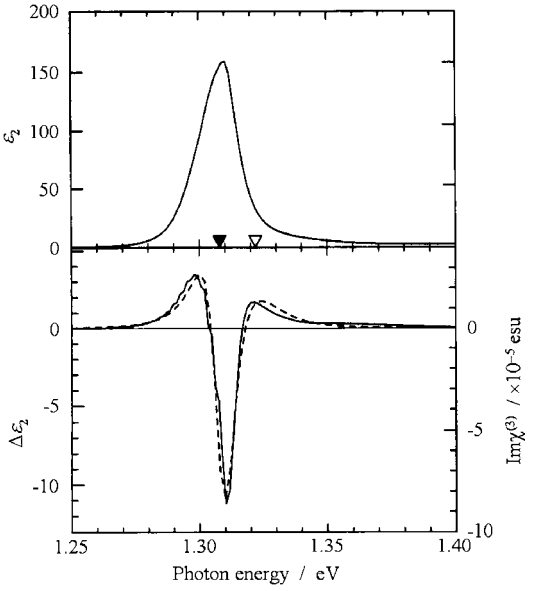

Figure 5. ε_2 and Im $\chi^{(3)}$ spectra at 77 K of $[Ni(chxn)_2Br]Br_2$. Filled and open triangle indicate the energies of the first ($\hbar\omega_1$) and second ($\hbar\omega_2$) excited states.

sional space can enhance $\chi^{(3)}$. Two types of chemically synthesized quantum wires have been extensively studied: band insulators of silicon polymers,[27] and Peierls insulators of π-conjugated polymers and platinum halides.[28] However, there had been no spectroscopic studies of 1D Mott insulators to evaluate nonlinear optical response.

We have measured the $\chi^{(3)}$ spectrum of this compound using electromodulation spectroscopy, which measures electric-field-induced change of optical reflectivity (ΔR). We have obtained the imaginary part of the $\chi^{(3)}$ spectrum (Im $\chi^{(3)}$) by the Kramers–Kronig transformation of $\Delta R/R$ to obtain the $\Delta\varepsilon_2$ spectrum and using the relation $\Delta\varepsilon_2 = 3\,\mathrm{Im}\,\chi^{(3)}E^2$.

Figure 5 shows ε_2 and Im $\chi^{(3)}$ ($\Delta\varepsilon_2$) spectra at 77 K of $[Ni(chxn)_2Br]Br_2$. In the Im $\chi^{(3)}$ spectrum, positive and negative components appear alternately as the photon energy increases. Such an oscillating structure can be explained by assuming three distinct states, that is, the ground state, one-photon allowed state, and one-photon forbidden state. By the applied electric field, the one-photon allowed state shows a red shift by the Stark effect, which leads to the increase of absorption at the lower energy side of the CT transition and decrease at the higher energy side. Therefore, this effect affords the first derivative shape of the $\Delta\varepsilon_2$ spectrum. Meanwhile, one-photon forbidden state is partially allowed, which affords an increase of absorption at the higher-energy side.

In this case, $\chi^{(3)}$ is given by perturbation theory. The main term dominating the spectral shape of $\chi^{(3)}$ is expressed as follows[29]

$$\chi^{(3)} = \frac{Ne^4}{3\varepsilon_0\hbar^3} \frac{\langle 0|x|1\rangle\langle 1|x|2\rangle\langle 2|x|1\rangle\langle 1|x|0\rangle}{(\omega_1 - \omega - i\gamma_1)(\omega_2 - \omega - i\gamma_2)(\omega_1 - \omega - i\gamma_1)} \quad (4)$$

where $|0>$, $|1>$, and $|2>$ show the ground state, one-photon allowed state and the one-photon forbidden state, respectively. $\omega_{1,2}$ and $\gamma_{1,2}$ are the energies and the damping factors for the excited states $|1>$ and $|2>$, respectively. More exact $\chi^{(3)}$ is

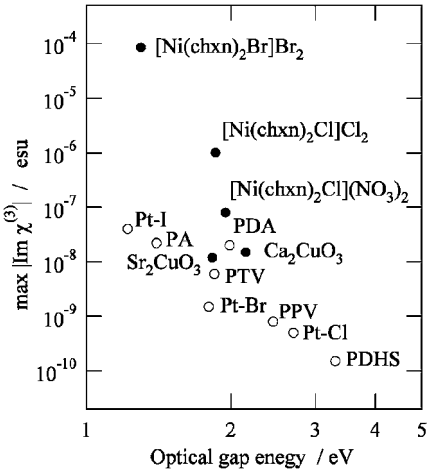

Figure 6. Maximum value of Im $\chi^{(3)}$ of a series of 1D compounds as a function of the optical gap energy. PDHS: polydihexylsilane, PA: polyacetylene, PDA: polydiacetylene, PTV: polythienylvinylene, PPV: poly(*p*-phenylenevinylene). Pt–I: $[Pt(en)_2][Pt(en)_2I_2](ClO_4)_4$, Pt–Br: $[Pt(en)_2][Pt(en)_2Br_2]$ $(ClO_4)_4$, Pt–Cl: $[Pt(en)_2][Pt(en)_2Cl_2](ClO_4)_4$. Open circles show the maximum values of Im $\chi^{(3)}$ of band insulators and Peierls insulators. Filled circles show those of Mott insulators.

composed of 12 independent terms including this equation. We carried out a parameter fitting (dashed line) and obtained a gigantic max $|\mathrm{Im}\,\chi^{(3)}|$ value ($=9\times10^{-4}$ esu at 1.31 eV).

Figure 6 shows a comparison of the maximum values of $|\mathrm{Im}\,\chi^{(3)}|$ as a function of optical gap energies obtained by electromodulation method. The maximum $|\mathrm{Im}\,\chi^{(3)}|$ values of band insulators such as polydihexylsilane (PDHS), polydiacetylene (PDA),[27] and Peierls insulators such as π-conjugated polymers and platinum halides[28] are ca. 10^{-10} to 10^{-7}. On the other hand, Mott-insulators showed much larger $\chi^{(3)}$ values than those of the other two types of 1D compounds.

By analyzing the spectrum in detail, it has been clarified that there are two factors in the strong enhancement of $\chi^{(3)}$ in the present compound; 1. large transition dipole moments ($<0|x|1>$ and $<1|x|2>$). 2. small energy splitting between ω_1 and ω_2 ($\approx$0.01 eV).

Photoluminescence is a powerful probe to investigate the electronic structure of excited states and their dynamics. Although photoluminescence, as relaxation processes, in Peierls-distorted (mixed-valence) MX-chain compounds have been extensively studied,[5] the processes in $[Ni(chxn)_2Br]Br_2$. are not clarified. We have studied luminescence properties of the non-Peierls MX-chain system $[Ni(chxn)_2Br]Br_2$.[30]

Figure 7 shows the temperature dependence of luminescence spectra with excitation energy $E_{ex} = 1.96$ eV. Large and small broad peaks were observed at 1.3 and 1.4 eV, respectively. It was reported that an intense band was observed at 1.3 eV in the optical conductivity spectrum,[10] being accounted for to be a LMCT transition (Br^-, $Ni^{3+} \rightarrow Br^0$, Ni^{2+}). The luminescence peak observed at 1.3 eV is, therefore, considered to be a relaxation of a LMCT exciton state (Br^0, $Ni^{2+} \rightarrow Br^-$, Ni^{3+}). This luminescence exhibits no or little Stokes shift, showing that the LMCT exciton is not easily relaxed into a self-trapped state. This is a good contrast to a relaxation process of the CT exciton state (M^{3+}, $M^{3+} \rightarrow M^{4+}$, M^{2+}) in Peierls-distorted MX-chain

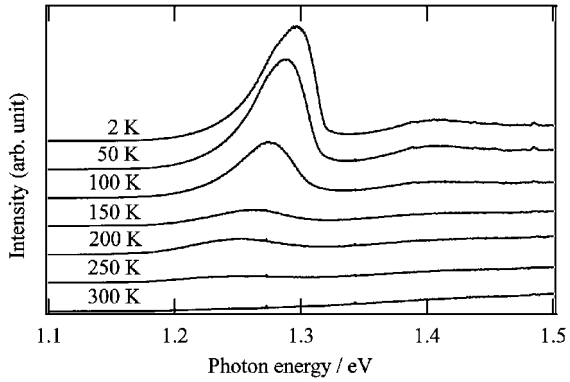

Figure 7. Temperature dependence of luminescence spectra in $[Ni(chxn)_2Br]Br_2$ with an excitation energy $E_{ex} = 1.96\,eV$.

system of M = Pd and Pt. These Pt and Pd compounds show large Stokes shifts due to the strong electron–lattice interaction because bridging halide ions X^- are quite sensitive to the charge of metal ions. On the other hand in $[Ni(chxn)_2Br]Br_2$, because the bridging bromine, which is neutral (Br^0) when the LMCT occurs, is insensitive to the charge at Ni ions, this compound showed almost no Stokes shift, indicating that the electron–lattice interaction (S) of this system is small or suppressed by some reason. More detailed studies have been recently made on the time dependence of the photoluminescence[31] as well as theoretical research.[32]

The peaks at 1.3 and 1.4 eV gradually disappear with temperature. This shows that the deactivation process continuously changes from luminescence to thermal relaxation. The peak at 1.3 eV slightly shifts to low energy with temperature. This slight shift might be accounted for as follows: The Ni–Br distance is expected to become longer with temperature, resulting in a decrease of the separation of Br^- $3p_z$ and Ni^{3+} $3d_{z^2}$ orbitals.

♦ Recent Progress in Ni Compounds

Fabrication of Optical Thin Films by Introducing Long Alkyl Chains

In the last section, we have shown the gigantic $\chi^{(3)}$ value measured by electromodulation method. For the application of optical device using $\chi^{(3)}$, however, it is necessary to obtain optical thin films. We have recently synthesized a new bromo-bridged Ni compound with a long alkyl chain in the in-plane ligand $[Ni(C_{14}\text{-en})_2Br]Br_2$ (C_{14}-en = 1,2-diaminohexadecane) in order to increase affinity to organic media.

Figure 8a shows a 1D chain structure of $[Ni(C_{14}\text{-en})_2Br]Br_2$. Although single crystals of this compound have not been obtained, we have confirmed that the 1D chain structure is sustained by Rietveld analysis of the powder X-ray diffraction pattern. The *n*-tetradecyl groups are bonded to the carbon atoms of ethylenediamine (en) ligand.

We fabricated the optical thin film by blending this compound to poly(methyl methacrylate) (PMMA) in chloroform and spin-coating on a CaF_2 substrate. Figure 8b shows a photograph of the optical thin film and absorption spectrum of the optical thin film. The spectral shape of this film is almost the same as that of $[Ni(chxn)_2Br]Br_2$, which is obtained by the Kramers–Kronig transformation of the single-crystal reflectivity spectrum ($Abs_{iso} = (2Abs_{\perp} + Abs_{//})/3$).

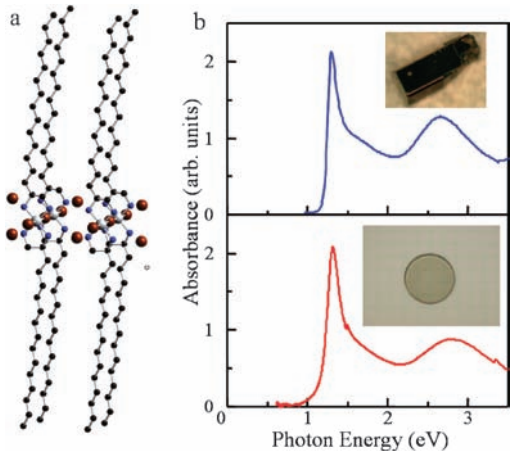

Figure 8. a) Crystal structure of $[Ni(C_{14}\text{-en})_2Br]Br_2$. Half of the disordered alkyl chain is omitted for clarity. Gray: Ni, Brown: Br, Blue: N, Black: C. b) Optical absorption spectrum of $[Ni(C_{14}\text{-en})_2Br]Br_2$ (lower) together with optical conductivity spectrum of $[Ni(chxn)_2Br]Br_2$ (upper). Insets shows a photograph of a single crystal of $[Ni(chxn)_2Br]Br_2$ (upper) and optical thin film of $[Ni(C_{14}\text{-en})_2Br]Br_2$ (lower).

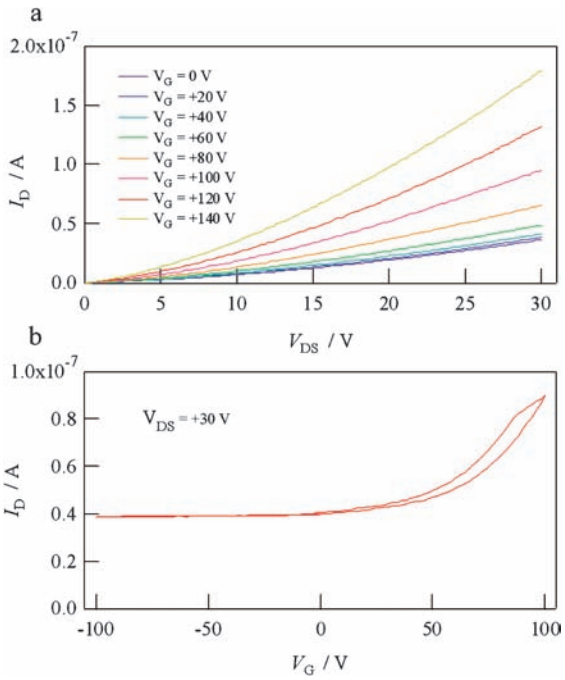

Figure 9. Output characteristics (a) and transport characteristics (b) in $[Ni(S,S\text{-bn})_2Br]Br_2$.

In order to investigate the potential of the $[Ni(C_{14}\text{-en})_2Br]Br_2$ film as a nonlinear optical medium, we measured the real and imaginary parts of $\chi^{(3)}$ by the Z-scan method, which is a representative method to estimate optical nonlinearity. By the Z-scan measurement, quite large values of $\chi^{(3)}$ were obtained ($\mathrm{Re}\,\chi^{(3)} = -1.5 \times 10^{-9}$ and $\mathrm{Im}\,\chi^{(3)} = 0.56 \times 10^{-9}$ esu at 1550 nm). In addition, it has been shown that this compound has a quite short lifetime of the photoexcited state (less than 1 ps) by measuring time dependence of absorption spectrum (pump-probe method), indicating that an optical

switching or modulation of more than $1\,\mathrm{T\,bit\,s^{-1}}$ is possible. Therefore, this optical thin film has very good potential as an optical switching medium.

Electrostatic Carrier Doping by Introducing to a FET Device

As we mentioned in the introduction, halogen-bridged Ni compounds have been interested as a 1D model of high T_c copper oxide superconductors because the band structures of these compounds are quite analogous to La_2CuO_4, which is the mother compound of high T_c copper oxide superconductor $La_{2-x}Sr_xCuO_4$, except for their dimensionality. Although many attempts have been made at carrier doping chemically, that has not been so far achieved because of the difficulty of chemical modification. Recently, we have synthesized the novel bromo-bridged Ni^{III} compound $[Ni(S,S\text{-bn})_2Br]Br_2$ (S,S-bn = 2S,3S-diaminobutane) and succeeded in electrostatic carrier doping by using a field-effect-transistor (FET) device for the first time.[33]

Figure 9a displays a plot of drain current (I_D) as a function of drain–source voltages (V_{DS}) (output characteristic) for various applied gate voltages (V_G) in this device at 77 K. I_D increased with increasing V_G in the positive voltage region, namely, n-type semiconductor behavior. On–off ratio was quite small because this compound is naturally electron doped. On–off ratio gradually decreased with increasing temperature because off-current is increased with temperature. No anomaly of FET properties due to spin-Peierls transition was observed. Figure 9b shows a plot of I_D as a function of V_G (transport characteristic) for various V_{DS} at 77 K. Output characteristics show neither linear nor saturated properties within the measured voltage range, and, therefore, carrier mobility cannot be evaluated.

♦ Summary and Outlook

We have described the structure, physical properties, and electronic structure of halogen-bridged 1D Ni^{III} compound $[Ni(chxn)_2Br]Br_2$, which is representative of 1D strongly correlated electron systems. In addition, we have introduced recent progress in our study of Ni^{III} compounds such as fabrication of optical thin films and electrostatic carrier doping.

In the past two decades, the chemistry and physics of strongly correlated electron systems has been extensively developed, e.g., superconductivity in copper oxides and gigantic third-order optical nonlinearity in the present Ni^{III} compounds. 1D compounds with strong electron correlation have good potential in physical properties such as conductive, optical, dielectric, and magnetic properties, and further progress will be made in the near future.

The present studies were made by collaboration with Mr. S. Tao, Dr. H. Matsuzaki, and Profs. H. Kishida and H. Okamoto in the University of Tokyo (Optical), Profs. H. Kitagawa and R. Ikeda at Kyushu University (NQR and photoluminescence), Drs. H. Ohtsu and M. Hasegawa at Aoyama-gakuin University (Ni compound with long alkyl chains), Profs. T. Takenobu and Y. Iwasa at Tohoku University (FET). We greatly acknowledge the collaborators.

This work was partly supported by a Grant-in Aid for Creative Scientific Research from the Ministry of Education, Culture, Sports, Science and Techonology.

References

1 H. Wolffram, Dissertation Königsberg, **1990**.
2 K. Nasu, *J. Phys. Soc. Jpn.* **1983**, *52*, 3865; S. M. Weber-Milbrodt, J. T. Gammel, A. R. Bishop, E. Y. Lor, Jr., *Phys. Rev. B* **1992**, *45*, 6435; K. Iwano, K. Nasu, *J. Phys. Soc. Jpn.* **1992**, *61*, 1380.
3 M. Tanaka, S. Kurita, T. Kojima, Y. Yamada, *Chem. Phys.* **1984**, *91*, 257; Y. Wada, T. Mitani, M. Yamashita, T. Koda, *J. Phys. Soc. Jpn.* **1985**, *54*, 3143.
4 R. J. H. Clark, M. L. Franks, W. R. Trumble, *Chem. Phys. Lett.* **1976**, *41*, 287; R. J. H. Clark, M. Kurmoo, D. N. Mountney, H. Toftlund, *J. Chem. Soc., Dalton Trans.* **1982**, 1851; R. J. H. Clark, *Chem. Soc. Rev.* **1990**, *19*, 107.
5 H. Tanino, K. Kobayashi, *J. Phys. Soc. Jpn.* **1983**, *52*, 1446.
6 H. Okamoto, T. Mitani, K. Toriumi, M. Yamashita, *Phys. Rev. Lett.* **1992**, *69*, 2248; H. Okamoto, M. Yamashita, *Bull. Chem. Soc. Jpn.* **1998**, *71*, 2023.
7 M. Yamashita, Y. Nonaka, S. Kida, Y. Hamaue, R. Aoki, *Inorg. Chim. Acta* **1981**, *52*, 43.
8 G. C. Papavassiliou, D. Z. Layek, *Z. Naturforsch., B: Anorg. Chem., Org. Chem.* **1982**, *37B*, 1406.
9 K. Toriumi, Y. Wada, T. Mitani, S. Bandow, M. Yamashita, Y. Fujii, *J. Am. Chem. Soc.* **1989**, *111*, 2341.
10 H. Okamoto, Y. Shimada, Y. Oka, A. Chainani, T. Takahashi, H. Kitagawa, T. Mitani, K. Toriumi, K. Inoue, T. Manabe, M. Yamashita, *Phys. Rev. B* **1996**, *54*, 8438.
11 H. Okamoto, T. Mitani, K. Toriumi, M. Yamashita, *Mater. Sci. Eng., B* **1992**, *13*, L9; H. Okamoto, T. Mitani, *Prog. Theor. Phys.* **1993**, *113*, 191.
12 K. Nasu, *J. Phys. Soc. Jpn.* **1983**, *52*, 3865; K. Iwano, K. Nasu, *J. Phys. Soc. Jpn.* **1992**, *61*, 1380; S. M. Weber-Milbrodt, J. T. Gammel, A. R. Bishop, E. Y. Lor, Jr., *Phys. Rev. B* **1992**, *45*, 6435.
13 H. Kishida, H. Matsuzaki, H. Okamoto, T. Manabe, M. Yamashita, Y. Taguchi, Y. Tokura, *Nature* **2000**, *405*, 929.
14 H. Okamoto, K. Toriumi, T. Mitani, M. Yamashita, *Phys. Rev. B* **1990**, *42*, 10381.
15 S. Takaishi, Y. Tobu, H. Kitagawa, A. Goto, T. Shimizu, T. Okubo, T. Mitani, R. Ikeda, *J. Am. Chem. Soc.* **2004**, *126*, 1614.
16 J. C. Bonner, M. E. Fisher, *Phys. Rev.* **1964**, *135*, A640.
17 S. Eggert, I. Affleck, M. Takahashi, *Phys. Rev. Lett.* **1994**, *73*, 332.
18 H. G. Dehmelt, H. Krüger, *Z. Physik* **1951**, *129*, 401.
19 P. W. Smith, R. Stoessiger, *J. Chem. Soc. D* **1971**, 279.
20 *Nuclear Quadrupole Resonance Spectra Data Base*, Japan Association for International Chemical Information, April, **2003**.
21 H. Bayer, *Z. Physik* **1951**, *130*, 227; T. Kushida, G. B. Benedek, N. Bloembergen, *Phys. Rev.* **1956**, *104*, 1364.
22 C. H. Townes, B. P. Dailey, *J. Chem. Phys.* **1949**, *17*, 782; B. P. Dailey, C. H. Townes, *J. Chem. Phys.* **1955**, *23*, 118.
23 J. G. King, V. Jaccarino, *Phys. Rev.* **1954**, *94*, 1610.
24 K. Ito, D. Nakamura, Y. Kurita, K. Ito, M. Kubo, *J. Am. Chem. Soc.* **1961**, *83*, 4526.
25 D. Nakamura, Y. Kurita, K. Ito, M. Kubo, *J. Am. Chem. Soc.* **1960**, *82*, 5783.
26 R. Ikeda, D. Nakamura, M. Kubo, *J. Phys. Chem.* **1965**, *69*, 2101.
27 T. Hasegawa, Y. Iwasa, H. Sunamura, T. Koda, Y. Tokura, H. Tachibana, M. Matsumoto, S. Abe, *Phys. Rev. Lett.* **1992**, *69*, 668.
28 Y. Iwasa, E. Funatsu, T. Hasegawa, T. Koda, M. Yamashita, *Appl. Phys. Lett.* **1991**, *59*, 2219; W.-S. Fann, S. Benson, J. M. Madey, S. Etemad, G. L. Baker, F. Kajzar, *Phys. Rev. Lett.* **1989**, *62*, 1492; C. Bubeck, A. Kaltbeitzel, A. Grund, M. LeClerc, *Chem. Phys.* **1991**, *154*, 343; C. Halvorson, T. W. Hagler, D. Moses, Y. Cao, A. J. Heeger, *Chem. Phys. Lett.* **1992**, *200*, 364.
29 P. N. Bucher, D. Cotter, *The Elements of Nonlinear Optics*, Cambridge University Press, **1990**.
30 S. Takaishi, H. Kitagawa, R. Ikeda, *Mol. Cryst. Liq. Cryst.* **2002**, *379*, 279.
31 Y. Takahashi, T. Suemoto, *Phys. Rev. B* **2004**, *70*, 081101.
32 K. Iwano, M. Ono, H. Okamoto, *Phys. Rev. B* **2002**, *66*, 235103; K. Iwano, *Phys. Rev. B* **2006**, *73*, 035108.
33 S. Takaishi, M. Yamashita, H. Matsuzaki, H. Okamoto, H. Tanaka, S. Kuroda, A. Goto, T. Shimizu, T. Takenobu, Y. Iwasa, *Chem.—Eur. J.* **2008**, *14*, 472.